Cancer Therapy: Preclinical

Clinical Cancer Research

The Telomerase Antagonist, Imetelstat, Efficiently Targets Glioblastoma Tumor-Initiating Cells Leading to Decreased Proliferation and Tumor Growth

Calin O. Marian[1], Steve K. Cho[2,6], Brian M. Mcellin[2,6], Elizabeth A. Maher[4,6], Kimmo J. Hatanpaa[3,6], Christopher J. Madden[5,6], Bruce E. Mickey[5,6], Woodring E. Wright[1], Jerry W. Shay[1], and Robert M. Bachoo[2,6]

Abstract

Purpose: Telomerase activity is one of the hallmarks of cancer and is a highly relevant therapeutic target. The effects of a novel human telomerase antagonist, imetelstat, on primary human glioblastoma (GBM) tumor-initiating cells were investigated *in vitro* and *in vivo*.

Experimental Design: Tumor-initiating cells were isolated from primary GBM tumors and expanded as neurospheres *in vitro*. The GBM tumor-initiating cells were treated with imetelstat and examined for the effects on telomerase activity levels, telomere length, proliferation, clonogenicity, and differentiation. Subsequently, mouse orthotopic and subcutaneous xenografts were used to assess the *in vivo* efficacy of imetelstat.

Results: Imetelstat treatment produced a dose-dependent inhibition of telomerase (IC_{50} 0.45 μmol/L). Long-term imetelstat treatment led to progressive telomere shortening, reduced rates of proliferation, and eventually cell death in GBM tumor-initiating cells. Imetelstat in combination with radiation and temozolomide had a dramatic effect on cell survival and activated the DNA damage response pathway. Imetelstat is able to cross the blood-brain barrier in orthotopic GBM xenograft tumors. Fluorescently labeled GBM tumor cells isolated from orthotopic tumors, following systemic administration of imetelstat (30 mg/kg every day for three days), showed ~70% inhibition of telomerase activity. Chronic systemic treatment produced a marked decrease in the rate of xenograft subcutaneous tumor growth.

Conclusion: This preclinical study supports the feasibility of testing imetelstat in the treatment of GBM patients, alone or in combination with standard therapies. *Clin Cancer Res; 16(1); 154–63. ©2010 AACR.*

Malignant gliomas are highly invasive and neurologically destructive tumors and are considered among the deadliest types of human cancer (1). In glioblastoma multiforme (GBM), the prognosis remains poor with 2-year survival of less than 5% (2). Improvements in surgery, radiation, and chemotherapy have seen modest gains in long-term survival, measured in months. With the current standard of care, which includes maximal surgical resection (when possible), localized radiation (50-60 Gy), and chemotherapy (temozolomide), the median survival is only 14.6 months (3).

Recent genomic studies have unveiled a highly complex picture of chromosomal amplifications and deletions, genetic mutations, and epigenetic modifications, which underscore the malignant behavior of GBM (4–6). Despite these significant advances in our basic understanding of GBM, the overall response rates to molecular targeted therapies have been disappointing (7), with perhaps the only exception being antiangiogenesis inhibitors (8). In addition to identifying novel therapeutic targets for a malignancy with a highly disorganized genome, there is also recent evidence showing that rare populations of GBM cells possess an inexhaustible ability to self-renew and proliferate (9–11). Operationally defined as cancer stem cells (or tumor-initiating cells), such cells may be especially resistant to conventional chemotherapies and ionizing radiation (12). There is considerable controversy over whether a single cell marker (such as CD133/prominin 1) can prospectively identify the tumor-initiating population in every tumor (13, 14). However, there is general agreement that GBM tumors cells, which can be propagated *in vitro* as nonadherent neurospheres and produce intracranial tumors, retain the genotype and phenotype of the patient's

Authors' Affiliations: Departments of [1]Cell Biology, [2]Neurology, [3]Pathology, [4]Internal Medicine, and [5]Neurosurgery, and [6]Annette G. Strauss Center for Neuro-Oncology, University of Texas, Southwestern Medical Center, Dallas, Texas

Note: Supplementary data for this article are available at Clinical Cancer Research Online (http://clincancerres.aacrjournals.org/).

C.O. Marian and S.K. Cho contributed equally to this research. R.M. Bachoo and J.W. Shay are co-senior contributors.

Corresponding Authors: Jerry W. Shay, Department of Cell Biology, Texas Southwestern Medical Center, 5323 Harry Hines Boulevard, Dallas, TX 75390-9039. Phone: 214-648-3282; Fax: 214-648-8694; E-mail: Jerry.Shay@UTSouthwestern.edu or Robert M. Bachoo. Phone: 214-645-6309; E-mail: Robert.Bachoo@UTSouthwestern.edu.

doi: 10.1158/1078-0432.CCR-09-2850

Translational Relevance

Glioblastoma is one of the most lethal human cancers, and the chemotherapeutic options are still limited by the reduced capacity of drugs to penetrate the blood-brain barrier. Cancer relapse is believed to be caused by small populations of tumor-initiating cells, which can escape conventional therapies. Imetelstat is a novel telomerase inhibitor that inhibits telomerase and induces telomere shortening in glioblastoma tumor-initiating cells, in addition to the bulk tumor mass. This preclinical study shows that imetelstat is a highly efficient and specific agent, both *in vitro* and in mouse orthotopic primary glioma xenografts. Imetelstat not only penetrates the blood-brain barrier but also shows increased efficacy in combination with ionizing radiation and temozolomide, the current standard of care for glioblastoma. The experimental data support the future implementation of imetelstat in clinical studies for glioblastoma.

original tumor (15, 16). As such, effective therapies for GBM may benefit from targeting specifically these cells to achieve a more durable tumor response.

Reactivation of telomerase activity is perhaps the single most consistent feature of the cancer phenotype, representing an almost obligate requirement for tumor growth, and therefore represents a potentially effective cancer therapeutic target (17). Normal brain tissues do not express telomerase activity (18–21), with the exception of a small population of neural stem cells, which may persist in the adult human brain (22). Several other reports have established a correlation between telomerase activity and histologic grade of gliomas (23, 24). Over the past decade, an extensive body of basic research into the mechanisms of telomere regulation has led to the identification of telomerase inhibitors (25), which may provide an effective, almost universal, cancer therapeutic strategy.

Imetelstat (GRN163L, Geron Corporation) is a short-chain oligonucleotide with high affinity and specificity for the template region of the RNA component of telomerase (hTR or hTERC). Imetelstat inhibits telomerase activity and has shown a highly favorable pharmacokinetic and minimal side-effect profile in early phase I clinical trials. The chemical makeup of this oligonucleotide (*thio*-phosphoramidate) confers high resistance to nuclease digestion in blood and tissues, and due to its 5′ lipid chain (palmitoyl), the molecule has excellent cellular and tissue penetration and retention properties (26). Importantly, imetelstat is a telomerase antagonist (not antisense that targets mRNA), and its mechanism of action is competitive with telomere binding, leading to inhibition of telomerase and progressive telomere shortening.

Here, we report that imetelstat produces a dose-dependent, reversible inhibition of telomerase activity in primary GBM tumor-initiating cells. Long-term exposure of primary GBM neurosphere cultures to imetelstat produced telomere attrition, growth arrest, and eventually cell death. When administered i.p. at clinically relevant doses, imetelstat was able to cross the blood-brain barrier and block telomerase activity of orthotopic human GBM xenograft tumors in nude mice. In addition, it produced a marked decrease in the rate of subcutaneous xenograft tumor growth. Taken together, our results strongly support the feasibility of using imetelstat in the treatment of GBM patients.

Materials and Methods

Isolation of GBM tumor-initiating cells. Tumor samples were obtained from consenting patients at the University of Texas Southwestern Medical Center (Dallas, TX) with the approval of the Institutional Review Board. Tumor tissues were dissociated, then cultured at clonal density in serum-free defined medium and/or labeled with a CD133 antibody (293C3-PE, Miltenyi Biotec) for subsequent sorting with a FACSAria apparatus (BD Biosciences). The GBM primary cells were maintained as nonadherent neurospheres in a humidified atmosphere (5% CO_2, 37 °C) in a chemically defined serum-free DMEM/F-12 (Cellgro), consisting of human recombinant epidermal growth factor (20 ng/mL; Sigma), basic fibroblast growth factor (20 ng/mL; Upstate), B27 supplement (1×; Invitrogen), insulin-transferrin-selenium-X (1×; Invitrogen), and penicillin-streptomycin (100 units/mL, 100 μg/mL; HyClone).

Estimation of telomerase activity and telomere lengths. The telomeric repeat amplification protocol (TRAP) was used to measure the telomerase activity (TRAPeze kit, Chemicon) according to the manufacturer's instructions. The telomerase products (6-bp ladder) and the 36-bp internal control [internal telomerase amplification standard (ITAS)] bands were quantified using the AlphaImager 2000 software (Alpha Innotech Corporation). Relative telomerase activity was calculated as the intensity ratio of the TRAP ladder to that of the ITAS band (relative intensity of each sample was normalized to that of the positive control).

Total DNA was extracted using the DNeasy Blood and Tissue Kit (Qiagen Sciences). One microgram of total DNA was used for the terminal restriction fragment (TRF) assay as previously described (27). The gel was exposed to a phosphor screen overnight and analyzed using the Typhoon Trio Variable Mode Imager (Amersham Biosciences).

Imetelstat treatment and proliferation assays. Neurospheres were passaged every 7 d to ensure that their size did not exceed the limit of diffusion (<150 μm) and/or to refresh growth factor–supplemented medium. Imetelstat and mismatch control oligonucleotide (5′-palm-TAGGTGTAAGCAA-NH_2-3′) were provided by Geron Corporation. For the viability assay of cells treated with imetelstat for extended periods of time, the Live/Dead

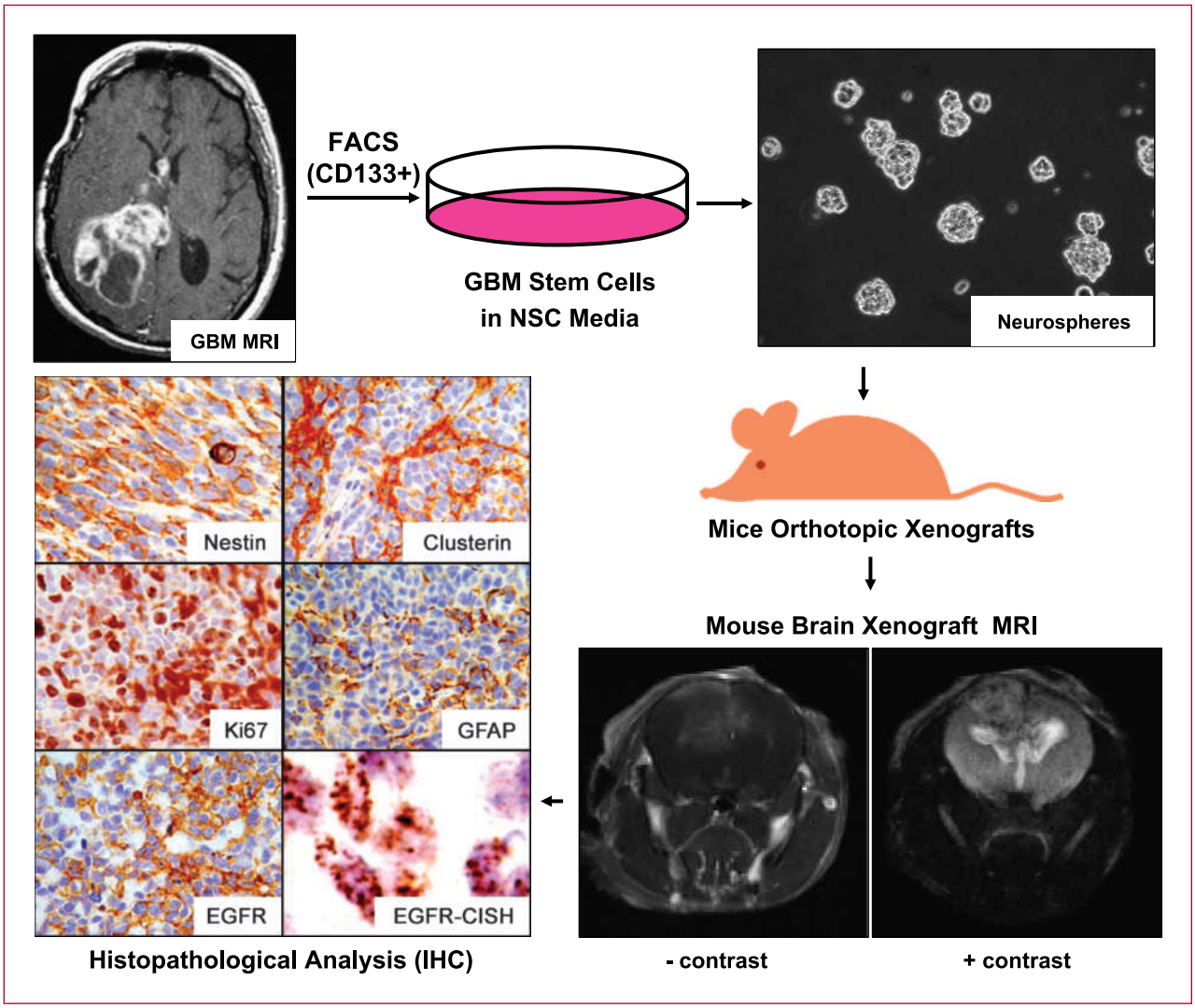

Fig. 1. Isolation and characterization of primary GBM tumor-initiating cells. Fresh primary GBM samples were dissociated and propagated as nonadherent neurospheres in serum-free defined medium. Orthotopic injection with dissociated neurosphere cells (5×10^4 per mouse) produced a neurologically symptomatic, T_1-contrast enhancing tumor mass following a latency of 8 to 10 wk. Histopathologic features of the tumor were consistent with high-grade glioma, including GFAP positivity, diffuse infiltration, high MiB-1 index (Ki67 positive), and areas of neovascularization. Immunohistochemistry (*IHC*) analysis confirmed EGFR overexpression. Chromagen-based *in situ* hybridization (*CISH*) indicated increased EGFR copy number in the orthotopic tumors. Orthotopic tumors also showed a heterogeneous mix of nestin-positive tumor cells (neural stem/progenitor marker) intermingled with clusterin-positive cells (astrocyte marker).

kit (Invitrogen) was used according to the manufacturer's recommendations.

The proliferation assays were done in 96-well tissue culture plates (BD Falcon) using MTT (Sigma-Aldrich). The MTT formazan produced in wells was solubilized with isopropanol 0.04 N HCl. Absorbance was measured on a Bio-Rad 680 microplate reader at a test wavelength of 570 nm and a reference wavelength of 630 nm. All proliferation experiments were done in triplicate.

Mouse xenograft experiments. To avoid contamination with host mouse cells and to noninvasively monitor intracranial tumor growth, we stably expressed monomeric Cherry (mCherry) red fluorescent protein and firefly luciferase (a gift from Dr. Tomoyuki Mashimo, University of Texas Southwestern, Internal Medicine Dallas, TX) in GBM cells. GBM tumor cells (1×10^5) were stereotactically injected into the right caudate of 6-wk-old nude mice. For the imetelstat experiments, each animal received the same total dose, but using a different schedule: (*a*) 30 mg/kg every 3 d, (*b*) 30 mg/kg every 2 d, and (*c*) 30 mg/kg each day. The mice that were clinically symptomatic for an intracranial mass were sacrificed by an overdose of anesthetic. The tumor was excised, dissociated, and washed, and mCherry-positive, live cells were gated from the control and the imetelstat

treatment groups on a Becton Dickinson FACSCalibur (BD Biosciences). For the subcutaneous xenografts, up to 1 million GBM tumor cells were injected into both flanks of 6- to 8-wk-old nonobese diabetic/severe combined immunodeficient mouse. The mice with subcutaneous tumors were separated into two cohorts (three mice each): vehicle and imetelstat. For both cohorts, imetelstat treatment was initiated when tumor volume reached 3 to 4 mm^3.

Orthotopic tumor histopathology and* in situ *hybridization. Mouse brains were fixed in 4% paraformaldehyde for 12 h, then cut into 5-μm sections for H&E staining. Chromogenic *in situ* hybridization for the epidermal growth factor receptor (*EGFR*) gene was done using a commercial probe and detection kit (SP-T Light 84-1300, Zymed). The primary antibodies and their dilutions were as follows: nestin (1:1,000; Abcam), clusterin (1:800; B5, Santa Cruz Biotechnology), Ki67 (prediluted; Ventana), GFAP (1:400; PP 040, Biocare Medical), and EGFR (prediluted; PharmDx, Dako). All immunostains were done in a Benchmark XT stainer (Ventana) using the CC1 pretreatment solution (95°C for 32 min; Ventana) and the XT-UltraView Universal 3,3′-diaminobenzidine detection system (Ventana). The sections were counterstained lightly with hematoxylin.

Bioluminescent imaging. Bioluminescent imaging of mice was done using the IVIS Lumina System (Xenogen Corp.) coupled to the LivingImage data acquisition software (Xenogen). D-luciferin (450 mg/kg in PBS in a total volume of 250 μL; Biosynthesis) was administered s.c. in the neck region; images were acquired between 10 and 20 min after luciferin administration and peak luminescent signal was recorded. The bioluminescent imaging signals emanating from the tumors were quantified by measuring photon flux within a region of interest using the LivingImage software package.

Results

Characterization of primary GBM tumor-initiating cells. To avoid the shortcomings associated with a single strategy of tumor-initiating cells isolation from primary tumors, we used three most common methods of enrichment: neurosphere formation, sorting based on the CD133 marker, and serial transplantation *in vivo*. Next, we tested the ability of these individual GBM neurosphere cells to produce intracranial tumors in nude mice. Orthotopic tumors were established by injecting 5×10^5 GBM tumor cells into the right striatum, and the mice were monitored clinically and by magnetic resonance imaging. Focal neurologic deficits consistent with an expanding intracranial mass were confirmed by magnetic resonance imaging scans (Fig. 1). Routine histologic analysis of the orthotopic tumors showed pathonemonic GBM features, including high MiB-1 index (Ki67 positive), nuclear atypia, diffuse infiltration, and modest angiogenesis (Fig. 1). One of the populations of neurospheres (initially enriched for $CD133^+$ cells by fluorescence-activated cell sorting) was chosen for all the subsequent studies, based on proliferation, tumor-initiating capacity, and ability to induce orthotopic xenografts similar, if not identical, to the human disease. To show that these GBM tumor-initiating cells were capable of multilineage differentiation, tumor cells were exposed to 2%

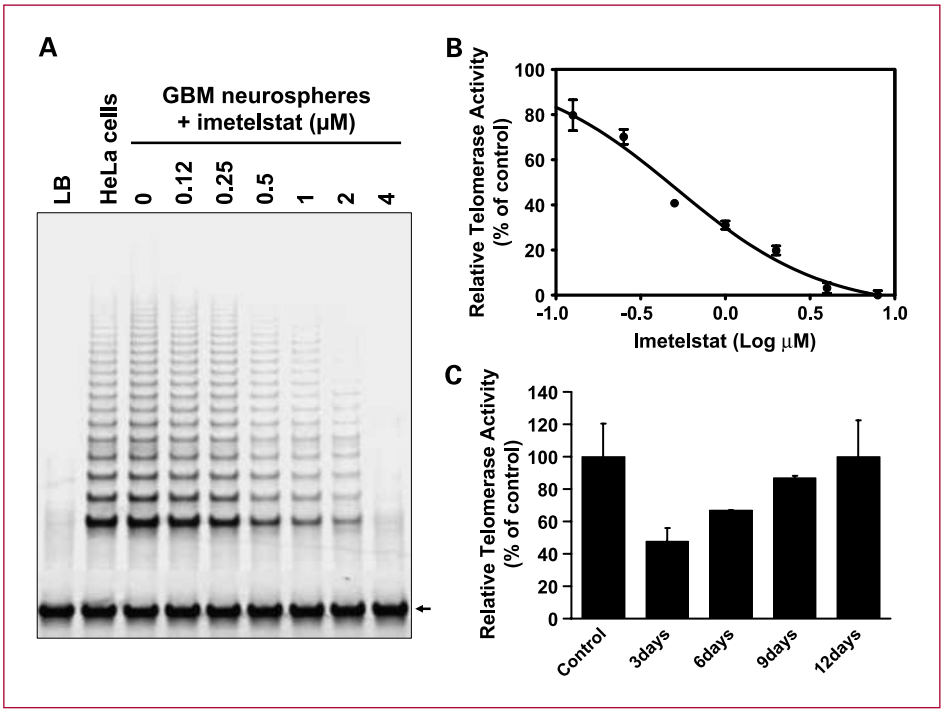

Fig. 2. Imetelstat inhibits telomerase activity in GBM tumor-initiating cells in a dose-dependent manner, which is reversed on drug removal. *A*, TRAP gel of the GBM neurospheres treated with various doses of imetelstat. *B*, the IC_{50} of telomerase activity inhibition is 0.45 μmol/L for this specific GBM tumor-initiating line. *C*, TRAP activity recovers to normal levels after imetelstat removal from the medium. The cells were treated with imetelstat for 72 h and then cultured in drug-free medium; samples were collected for TRAP every 3 d. Equal numbers of cells were used for the TRAP assay. HeLa cells lysate was used as a positive control. Columns, average data from three independent TRAP assays. Arrow, the ITAS used for quantitation.

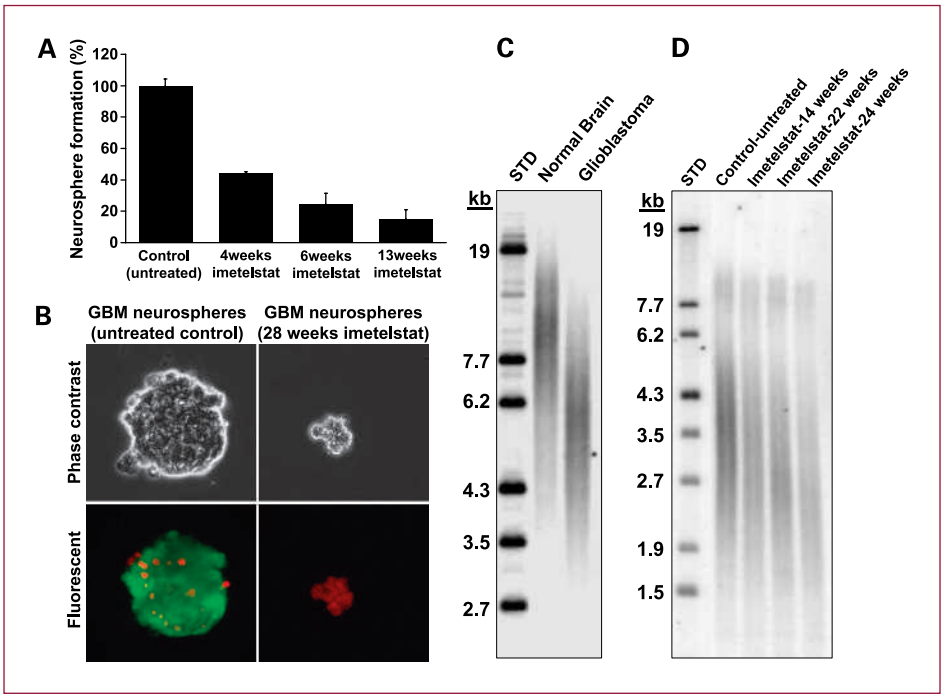

Fig. 3. Long-term treatment with imetelstat *in vitro* leads to decreased clonogenic capacity, telomere shortening, and cell death. *A*, clonogenic neurosphere formation assay of GBM tumor-initiating cells exposed to imetelstat. A total of 500 cells were plated on 10-cm dishes; fresh medium was exchanged after 5 d; and the neurospheres were counted after 10 to 14 d. *B*, live/dead assay on the long term-treated cells versus the untreated controls. Green cells, Calcein AM (live cells); red cells, ethidium homodimer (necrotic cells). *C*, TRF gel shows that GBM tumor cells have short telomeres (average of ~6 kb) compared with normal brain (~10-12 kb). *D*, TRF analysis of another primary glioma that has even shorter initial average telomere length (~3.5-4 kb) indicates progressive telomere shortening in GBM tumor-initiating cells treated *in vitro* twice a week with 2 μmol/L imetelstat.

FCS for 1 wk, as reported previously (9, 11). Quantitative reverse transcription-PCR results showed a marked downregulation of neuronal (MAP2 and NeuroD) and upregulation of mature astrocyte (clusterin and GFAP) genes, while downregulating CD133 (Supplementary Fig. S1A). The results confirmed that the GBM tumor-initiating cells maintained under neurosphere culture conditions expressed a neural stem cell–like phenotype and are capable of differentiation.

GBM tumor-initiating cells treated with imetelstat show a dose-dependent and reversible inhibition of telomerase activity. Having confirmed that the primary GBM cell line possessed tumor-initiating cell properties, we proceeded to test the telomerase antagonist imetelstat. Telomerase expression levels in the GBM tumor-initiating cells were similar to those in the HeLa cells used as positive controls (Fig. 2A). By contrast, normal adult human brain tissue, isolated from temporal lobe resections, had no detectable telomerase activity (data not shown).

Imetelstat inhibits the telomerase activity of GBM tumor-initiating cells *in vitro* in a dose-dependent fashion (Fig. 2A and B). At a dose of 0.45 μmol/L, imetelstat produced 50% inhibition of telomerase activity, and at 4 μmol/L produced ~100% inhibition (Fig. 2B). In contrast, the imetelstat mismatch control oligonucleotide had no effect on the levels of telomerase activity even at doses of up to 4 μmol/L (data not shown). The inhibition of telomerase activity produced by imetelstat was found to be entirely reversible following drug removal from the culture medium over a period of 12 days (Fig. 2C).

Prolonged telomerase inhibition leads to telomere shortening, progressive growth arrest, and eventual cell death. To test the effects of imetelstat on cell proliferation, GBM tumor-initiating cells were passaged in the presence of 2 μmol/L imetelstat. Over the first 4 weeks (~4 population doublings), imetelstat-treated and imetelstat-mismatch cultures showed no significant difference in proliferation but a significant decrease in their clonogenic ability (Fig. 3A). Thereafter, imetelstat-exposed cells showed a progressive decrease in the rate of proliferation, paralleled by a decrease in their capacity to form neurospheres when plated at low density (Fig. 3B). After approximately 20 population doublings (24 weeks of continuous imetelstat exposure), dissociated single tumor cells produced very small (<50 μm) neurospheres, which were ragged in appearance and largely positive for ethidium homodimer-1, indicating disrupted membrane integrity associated with ensuing cell death (see Fig. 3B). In contrast, all three replicates of control cultures continued to proliferate normally.

The experimental data confirmed that the telomeres of GBM tumors are shorter than normal brain telomeres (Fig. 3C). The TRF (telomere length) blot indicated that GBM tumor-initiating cells also have short telomeres (~3.5 kb), with two distinct subpopulations (Fig. 3D). The two distinct populations of telomeres (short and long) represent variations of telomere lengths in the same cell. This was confirmed by isolating several clones and each clone had a similar TRF pattern, indicating that one or a few telomeres are longer in these cells (data not shown), and with imetelstat treatment all telomeres show progressive shortening. The average telomere length of long-term imetelstat-treated GBM tumor-initiating cells showed a marked decline from ~3.5 to <2.0 kilobases

(Fig. 3D), whereas oligonucleotide mismatch–treated cultures showed no decline after 28 weeks of continuous treatment (data not shown). These results suggest that telomerase inhibition of rapidly expanding populations of GBM tumor cells exposed to imetelstat caused progressive telomere shortening, leading to cell cycle arrest and cell death.

Because telomere shortening and/or loss of telomerase activity in neuronal progenitors has been reported to promote neuronal differentiation (28, 29), we tested whether prolonged imetelstat exposure could trigger the differentiation of GBM tumor-initiating cells and, as a result, lead to cell cycle arrest/cell death. Systematic and quantitative analysis of multiple lineage specific markers, including markers for stem/progenitor cells (CD133 and nestin), neuronal lineage (Tuj1, MAP2, and NeuroD), and astrocyte markers (GFAP and clusterin), showed no evidence of differentiation (Supplementary Fig. S1B) as a result of imetelstat treatment.

***Addition of imetelstat to radiation and temozolomide increases therapeutic efficacy* in vitro.** Because the current standard of care for GBM patients (post-resection) is ionizing radiation and temozolomide, we tested whether imetelstat had any additive or synergistic effects when combined with these therapy regimens. GBM tumor-initiating cells that had been treated with imetelstat for 16 weeks showed a marked decrease in the rate of proliferation, due to progressive telomere shortening. The effect of imetelstat on these cells was further enhanced by treatment with temozolomide and irradiation (Fig. 4A), suggesting that addition of imetelstat to the standard of care may have some added therapeutic benefits.

Short-term treatment (72 hours) with imetelstat in combination with temozolomide also led to significant cytotoxicity in GBM tumor-initiating cells, but 5-Gy irradiation had little effect on cell survival or proliferation (Fig. 4B). The magnitude and rate of DNA double-strand breaks repair were quantitatively assessed by Western blot analysis of γH2AX and 53BP1 phosphorylation. GBM tumor-initiating cells irradiated with a total dose of 5 Gy in the presence and absence of imetelstat showed

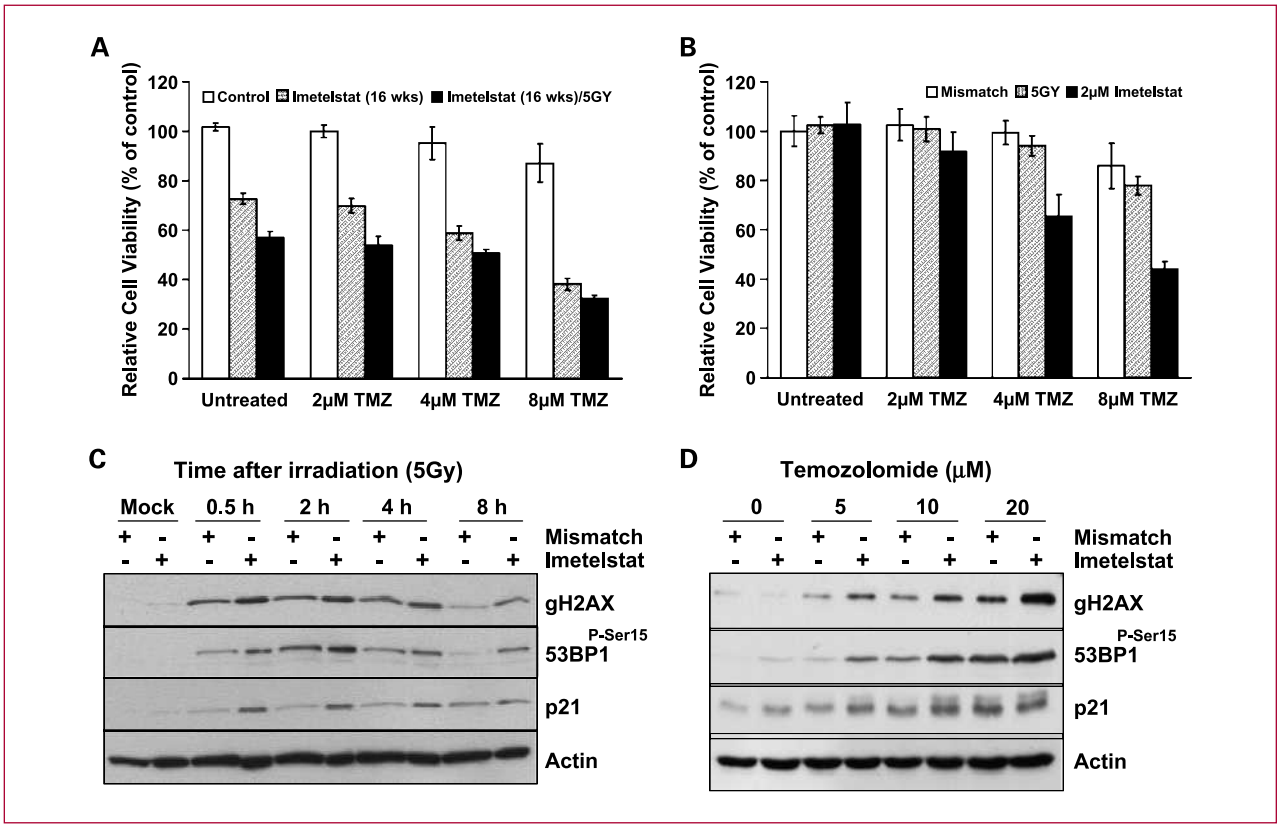

Fig. 4. Radiation therapy and temozolomide are more efficient on GBM tumor-initiating cells when used in combination with imetelstat. *A,* cell survival assay (MTT) done on cells treated with the telomerase inhibitor imetelstat (16 wk), temozolomide (*TMZ*), and irradiation (5 Gy). The data were normalized to the control, oligonucleotide mismatch–treated cells. *B,* addition of temozolomide to tumor cells pretreated with imetelstat for 72 h produced a marked effect on tumor cell viability ($P < 0.001$), as indicated by the MTT assay. Treatment with temozolomide alone or in combination with 5-Gy irradiation produced only a small decrease in tumor cell proliferation. *C,* Western blot of GBM tumor-initiating cells pretreated with imetelstat (72 h) followed by ionizing radiation (5 Gy) indicated an effect on DNA double-strand breaks as measured by increased γH2AX (Ser^{139}) and 53BP1 phosphorylation. *D,* Western blot of GBM tumor-initiating cells treated with a combination of imetelstat and temozolomide (5, 10, and 20 μmol/L) showed increased activation of γH2AX and 53BP1 phosphorylation compared with the mismatch controls.

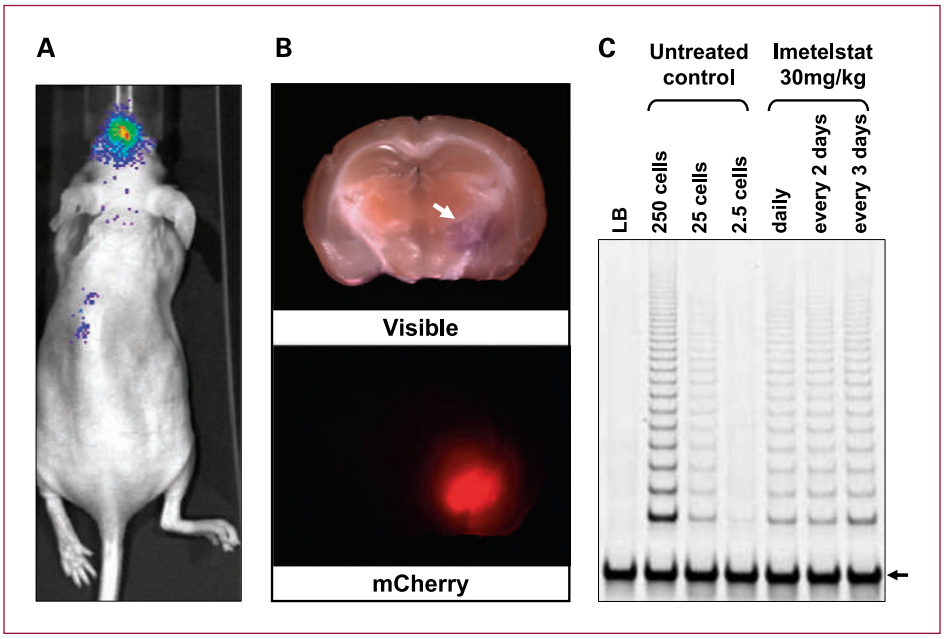

Fig. 5. Imetelstat penetrates the blood-brain barrier and inhibits telomerase activity in orthotopic xenograft tumors. *A*, bioluminescent imaging of mCherry/Luc–labeled GBM tumor-initiating cells implanted orthotopically in the brain of a nude mouse. *B*, macroscopic pathology of the mouse brain with the orthotopic tumor (*white arrow*). Fluorescent image of the mouse brain shows strong mCherry expression in tumor cells. *C*, TRAP assay of cells isolated by fluorescence-activated cell sorting from intracranial tumors of mice treated with imetelstat. Cell lysates corresponding to 250 cells were used for the imetelstat-treated samples. Arrow, ITAS control.

peak γH2AX and 53BP1 phosphorylation at 30 to 120 minutes and near-complete recovery by 8 hours (Fig. 4C). The levels of these proteins were significantly higher in the cells treated with imetelstat compared with the mismatch controls. Similarly, treatment with temozolomide over a dose range of 5, 10, and 20 μmol/L also showed marked activation of γH2AX and 53BP1 phosphorylation in the imetelstat-treated samples (Fig. 4D).

Imetelstat penetrates the blood-brain barrier and inhibits telomerase activity in a GBM orthotopic glioblastoma model. To accurately estimate telomerase activity in orthotopic GBM tumor cells following systemic treatment with imetelstat, we used tumor cells that were transduced with a firefly luciferase reporter as well as mCherry (Fig. 5A and B). We first established that in our orthotopic mouse tumors (Supplementary Fig. S2A and B), the microvasculature in regions of infiltrating tumor cells continued to express the tight junction–associated proteins ZO-1 and occludin (Supplementary Fig. S2C and D), which are critical for maintaining the blood-brain barrier (30). Double labeling with CD31 and smooth muscle antigen was used as an indicator that capillaries surrounded by infiltrating tumor cells retained normal pericyte coverage (Supplementary Fig. S2E). We also established that tumor-associated capillaries maintain normal astrocyte foot process coverage by detecting a normal pattern of aquaporin-4 immunofluorescence, which is exclusively localized to the astrocytic processes (Supplementary Fig. S2C and F). These results strongly indicate that the histopathology of these orthotopic GBM tumor cells was a near phenocopy of the clinical disease in humans, showing how diffusely infiltrating tumor cells can co-opt normal brain microcirculation, which severely limits penetration of most chemotherapeutic approaches.

The intracranial bioluminescence signal was used to monitor the overall orthotopic tumor size. At the end of each treatment schedule, the mice were sacrificed and mCherry-positive cells were isolated. At approximately 50% of the maximum tolerated intracranial tumor size (based on pilot studies), the mice were treated with 30 mg/kg imetelstat by i.p. injection using three different dosing schedules (see Materials and Methods). Telomerase activity was inhibited by 60% to 70% within 3 to 5 days, and no significant differences were observed between these three different dosing schedules (Fig. 5C). These results compare favorably with subcutaneous xenografts of GBM tumor cells treated with the same total dose of imetelstat, which showed similar telomerase inhibition (data not shown). The high levels of telomerase inhibition indicate that imetelstat can penetrate the blood-brain barrier and induce significant inhibition of telomerase activity in brain tumor xenografts.

In vivo *glioblastoma model shows inhibition of tumor growth in response to imetelstat treatment.* To test the effect of imetelstat on tumor growth *in vivo*, we established subcutaneous tumors in mice. Imetelstat led to a significant decrease in tumor size compared with the vehicle only–treated group (Fig. 6A). Based on the bioluminescent imaging data, there was a more than 10-fold difference in the average signal intensity between the imetelstat-treated animal group and the control group at the end of the 53 days of treatment (Fig. 6B). At the termination of the experiment (based on tumor volume and animal care policies), the tumors were excised and measured (by caliper) in their greatest length and width (Fig. 6A, *bottom*). The average tumor volume in the treated animals was more than 10-fold lower compared with

the control animals (data not shown). The growth rate of GBM subcutaneous tumors in the imetelstat cohort was significantly lower compared with the vehicle group (Fig. 6B). Taken together, these results suggest that imetelstat could be highly effective in reducing GBM tumor growth.

Discussion

Telomerase activity is a strong indicator of cellular malignancy (17), and in GBM tumors, high levels of telomerase expression correlate with tumor progression and poor prognosis (19–21, 31). Here, we report that a novel human telomerase antagonist, imetelstat, is a potent inhibitor of telomerase activity in primary human GBM tumor-initiating cells. The ability to target these crucial subpopulations of cells that evade conventional and targeted therapies could be a significant step in developing effective strategies for GBM treatment.

For this study, we used primary GBM tumor-initiating cells that produce orthotopic tumors with accurate GBM histopathology. The isolated tumor-initiating cells were also cultured as nonadherent neurospheres, conditions which maintain their stem-like properties (11, 13, 32). Imetelstat produced a dose-dependent, reversible inhibition of telomerase activity over a wide dose range that persists for several days, raising the possibility that the pharmacokinetics may be well suited for the clinical setting. The negative effect of imetelstat on proliferation was not evident until after approximately 15 to 20 population doublings, when progressive telomere attrition leads to the induction of DNA damage signaling, end-to-end fusions, and genetic instability, processes that can lead to apoptotic cell death.

Because tumor cells share the same telomere elongation machinery with normal proliferative stem-like cells, one major concern associated with the use of a telomerase inhibitors is the potential decline of regenerative capacity in normal stem cells. Such an adverse possibility is of particular concern for the organs with high rates of cellular turnover and especially relevant in elderly patients. Because telomere shortening occurs in most human tissues during aging and is accelerated in response to chronic diseases (33), it is important to determine the telomere length not only in tumor-initiating stem cells but also in normal stem cells. The results of our present studies clearly show that the average telomere lengths of GBM tumor cells are approximately three times shorter compared with normal human brain cells (~10 versus 3.5 kb). In principle, assuming equivalent rates of proliferation, this difference offers an ample therapeutic window to cause malignant tumor cells to undergo critical telomere shortening while telomeres in the normal stem cell compartment remain of adequate length. Moreover, following removal of imetelstat, telomerase activity rapidly recovers to normal levels, which suggests that potential adverse telomere shortening

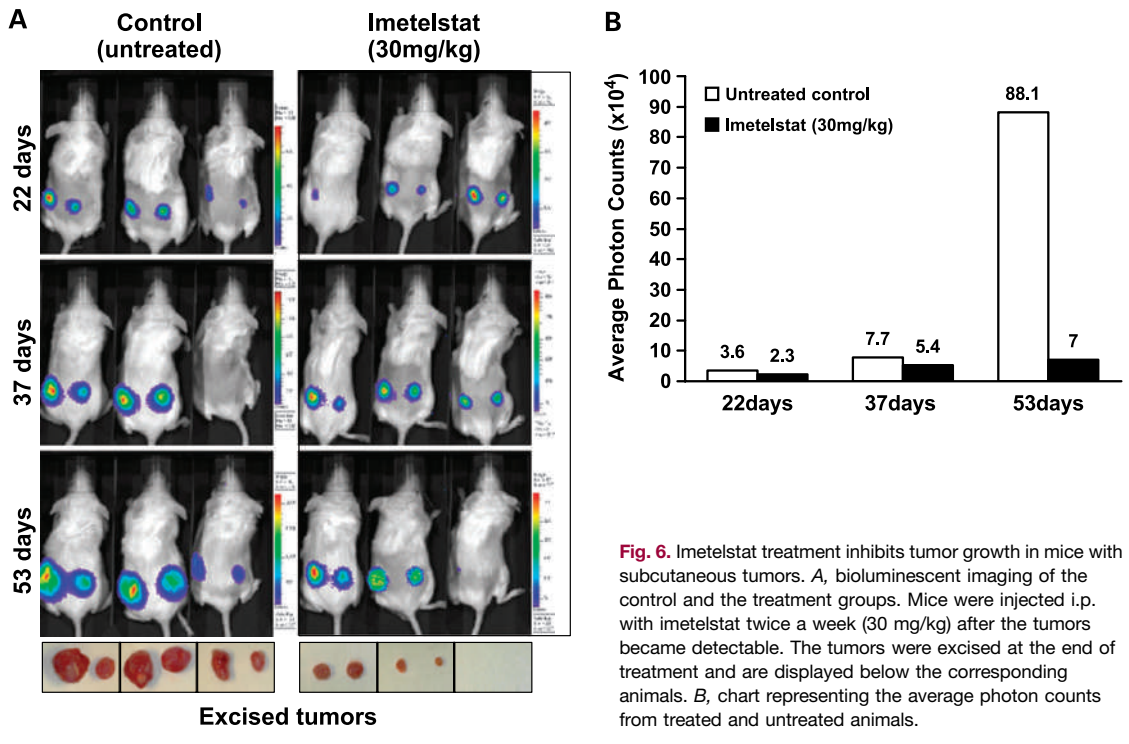

Fig. 6. Imetelstat treatment inhibits tumor growth in mice with subcutaneous tumors. *A*, bioluminescent imaging of the control and the treatment groups. Mice were injected i.p. with imetelstat twice a week (30 mg/kg) after the tumors became detectable. The tumors were excised at the end of treatment and are displayed below the corresponding animals. *B*, chart representing the average photon counts from treated and untreated animals.

in the normal stem cells may be reversible. Clearly, this is a significant advantage over conventional chemotherapies, which often produce irreversible damage to all proliferative cells including stem cells of renewal tissues.

Recent studies have shown that combination of temozolomide and ionizing radiation has some therapeutic benefits. We explored whether addition of imetelstat would increase the therapeutic potential of these agents and show that GBM neurosphere cells treated with imetelstat for long periods of time are more sensitive to ionizing radiation and temozolomide (Fig. 5A). Whereas the additive effects seen with temozolomide or ionizing radiation and long-term imetelstat-treated cultures were consistent with previous data on irradiated breast cancer cells (34), the effects of temozolomide on short-term imetelstat-treated cells were surprising because this combination led to increased toxicity in the absence of telomere shortening (Fig. 4B). This result seems to be specific for temozolomide because the cells irradiated with a dose of 5 Gy do not show significant cytotoxicity compared with the unirradiated controls, but we cannot exclude the possibility that GBM cells subjected to other ionizing radiation regimens may exhibit a similar response. One explanation for this mechanism of drug synergy may be that ionizing radiation and temozolomide induced telomeric DNA breaks that could not be repaired in the absence of telomerase, leading to an increased DNA damage response (Fig. 5B and C). Another explanation is that treatment with imetelstat may activate an elevated autophagy response in GBM cells. It is documented that temozolomide triggers GBM cell death by autophagy (35, 36), and some reports suggest that GBM tumor-initiating cells are resistant to the temozolomide-induced autophagy due to the downregulation of critical proteins (37). Interestingly, the gene encoding one of these autophagy proteins (*APG5*) was found to be significantly upregulated in myeloma cells treated with imetelstat (38). Moreover, it was shown that a conditionally replicating hTERT adenovirus can induce autophagic cell death in malignant glioma cells (39). Taken together, these data suggest that the telomere length–independent effects of imetelstat along with its primary effect on telomere elongation may be uniquely effective against GBM tumor-initiating cells.

One of the major challenges in brain tumor therapy remains the difficulty of delivering drugs across the blood-brain barrier. Building on previous biodistribution studies (40), our hypothesis was that imetelstat could penetrate the blood-brain barrier and efficiently inhibit telomerase in orthotopic GBM tumors. Despite strong evidence of tight junctions, our data clearly show for the first time that i.p. introduced imetelstat was able to penetrate the blood-brain barrier in sufficient intra-parenchymal concentration to block ~70% of telomerase activity in human GBM orthotopic xenograft cells.

The *in vitro* data indicated that GBM tumor-initiating cell must undergo at least 15 to 20 population doublings before significant telomere attrition may occur. Because in the orthotopic model 5×10^4 cells were injected into the brain, the total cell number following 20 population doublings would be 5×10^{10} cells, which would exceed the 1 to 2 mm^3 maximum tumor mass an adult mouse cranium can accommodate without brainstem compression, herniation, and death. For this reason, we used subcutaneous xenografts to investigate the *in vivo* effects of imetelstat on tumor growth rate and size because this model can accommodate much larger tumor volumes (2 cm^3) without significant morbidity. Furthermore, imetelstat penetration data show that telomerase inhibition of GBM tumors cells is very similar for the subcutaneous and intracranial tumors; therefore, the subcutaneous xenograft model is more than adequate for a therapeutic proof of concept. Drug treatment was initiated once the subcutaneous tumors were clearly visible (~1 mm) and the results show significant differences between the imetelstat- and vehicle-treated mice (Fig. 6). Regular monitoring of tumor size by bioluminescence initially showed little difference between the treated and the control cohorts, but as the tumor masses approached 25% of maximal tolerate size (500 mm^3), imetelstat-treated tumors were showing a significantly slower tumor growth, presumably due to a subset of tumor cells having undergone the required number of population doublings for critical telomere shortening. Most GBM patients undergo aggressive debulking resection (unless contraindicated by tumor location or other co-morbidities), which will ensure that there is sufficient space to permit tumor growth and erosion of telomeres to critical levels that trigger cellular quiescence and/or cell death. We predict an even greater therapeutic efficacy and perhaps a durable response when imetelstat is combined with radiation and temozolomide, which currently provides only a partial response. Taken together, the *in vitro* and *in vivo* data are encouraging for pursuing testing of imetelstat in GBM patients.

Disclosure of Potential Conflicts of Interest

No potential conflicts of interest were disclosed.

Acknowledgments

We thank Geron Corporation (Menlo Park, CA) for providing the imetelstat drug used in this study.

Grant Support

Supported in part by National Cancer Institute Specialized Programs of Research Excellence grants CA70907 and CA127297.

The costs of publication of this article were defrayed in part by the payment of page charges. This article must therefore be hereby marked *advertisement* in accordance with 18 U.S.C. Section 1734 solely to indicate this fact.

Received 10/24/09; accepted 12/3/09; published online 1/4/10.

References

1. Wen PY, Kesari S. Malignant gliomas in adults. N Engl J Med 2008; 359:492–507.
2. Buckner JC. Factors influencing survival in high-grade gliomas. Semin Oncol 2003;30:10–4.
3. Stupp R, Mason WP, van den Bent MJ, et al. Radiotherapy plus concomitant and adjuvant temozolomide for glioblastoma. N Engl J Med 2005;352:987–96.
4. Mulholland PJ, Fiegler H, Mazzanti C, et al. Genomic profiling identifies discrete deletions associated with translocations in glioblastoma multiforme. Cell Cycle 2006;5:783–91.
5. Marko NF, Toms SA, Barnett GH, Weil R. Genomic expression patterns distinguish long-term from short-term glioblastoma survivors: a preliminary feasibility study. Genomics 2008;91:395–406.
6. CancerGenomeAtlas. Comprehensive genomic characterization defines human glioblastoma genes and core pathways. Nature 2008;455:1061–8.
7. Furnari FB, Fenton T, Bachoo RM, et al. Malignant astrocytic glioma: genetics, biology, and paths to treatment. Genes Dev 2007;21:2683–710.
8. Jouanneau E. Angiogenesis and gliomas: current issues and development of surrogate markers. Neurosurgery 2008;62:31–50, discussion -2.
9. Piccirillo SG, Reynolds BA, Zanetti N, et al. Bone morphogenetic proteins inhibit the tumorigenic potential of human brain tumour-initiating cells. Nature 2006;444:761–5.
10. Dirks PB. Brain tumour stem cells: the undercurrents of human brain cancer and their relationship to neural stem cells. Philos Trans R Soc Lond B Biol Sci 2008;363:139–52.
11. Singh SK, Hawkins C, Clarke ID, et al. Identification of human brain tumour initiating cells. Nature 2004;432:396–401.
12. Bao S, Wu Q, McLendon RE, et al. Glioma stem cells promote radioresistance by preferential activation of the DNA damage response. Nature 2006;444:756–60.
13. Singh SK, Clarke ID, Terasaki M, et al. Identification of a cancer stem cell in human brain tumors. Cancer Res 2003;63:5821–8.
14. Wang J, Sakariassen PO, Tsinkalovsky O, et al. CD133 negative glioma cells form tumors in nude rats and give rise to CD133 positive cells. Int J Cancer 2008;122:761–8.
15. Lee J, Kotliarova S, Kotliarov Y, et al. Tumor stem cells derived from glioblastomas cultured in bFGF and EGF more closely mirror the phenotype and genotype of primary tumors than do serum-cultured cell lines. Cancer Cell 2006;9:391–403.
16. Tunici P, Bissola L, Lualdi E, et al. Genetic alterations and *in vivo* tumorigenicity of neurospheres derived from an adult glioblastoma. Mol Cancer 2004;3:25.
17. Shay JW, Wright WE. Telomerase: a target for cancer therapeutics. Cancer Cell 2002;2:257–65.
18. DeMasters BK, Markham N, Lillehei KO, Shroyer KR. Differential telomerase expression in human primary intracranial tumors. Am J Clin Pathol 1997;107:548–54.
19. Le S, Zhu JJ, Anthony DC, Greider CW, Black PM. Telomerase activity in human gliomas. Neurosurgery 1998;42:1120–4, discussion 4–5.
20. Huang F, Kanno H, Yamamoto I, Lin Y, Kubota Y. Correlation of clinical features and telomerase activity in human gliomas. J Neurooncol 1999;43:137–42.
21. Harada K, Kurisu K, Tahara H, Tahara E, Ide T, Tahara E. Telomerase activity in primary and secondary glioblastomas multiforme as a novel molecular tumor marker. J Neurosurg 2000;93:618–25.
22. Ostenfeld T, Caldwell MA, Prowse KR, Linskens MH, Jauniaux E, Svendsen CN. Human neural precursor cells express low levels of telomerase *in vitro* and show diminishing cell proliferation with extensive axonal outgrowth following transplantation. Exp Neurol 2000; 164:215–26.
23. Langford LA, Piatyszek MA, Xu R, Schold SC, Jr., Shay JW. Telomerase activity in human brain tumours. Lancet 1995;346:1267–8.
24. Falchetti ML, Larocca LM, Pallini R. Telomerase in brain tumors. Childs Nerv Syst 2002;18:112–7.
25. Harley CB. Telomerase and cancer therapeutics. Nat Rev 2008;8: 167–79.
26. Herbert BS, Gellert GC, Hochreiter A, et al. Lipid modification of GRN163, an N3′→P5′ thio-phosphoramidate oligonucleotide, enhances the potency of telomerase inhibition. Oncogene 2005;24:5262–8.
27. Gellert GC, Dikmen ZG, Wright WE, Gryaznov S, Shay JW. Effects of a novel telomerase inhibitor, GRN163L, in human breast cancer. Breast Cancer Res Treat 2006;96:73–81.
28. Kruk PA, Balajee AS, Rao KS, Bohr VA. Telomere reduction and telomerase inactivation during neuronal cell differentiation. Biochem Biophys Res Commun 1996;224:487–92.
29. Richardson RM, Nguyen B, Holt SE, Broaddus WC, Fillmore HL. Ectopic telomerase expression inhibits neuronal differentiation of NT2 neural progenitor cells. Neurosci Lett 2007;421:168–72.
30. Wolburg H, Lippoldt A. Tight junctions of the blood-brain barrier: development, composition and regulation. Vascul Pharmacol 2002; 38:323–37.
31. Chong EY, Lam PY, Poon WS, Ng HK. Telomerase expression in gliomas including the nonastrocytic tumors. Hum Pathol 1998;29:599–603.
32. Galli R, Binda E, Orfanelli U, et al. Isolation and characterization of tumorigenic, stem-like neural precursors from human glioblastoma. Cancer Res 2004;64:7011–21.
33. Aubert G, Lansdorp PM. Telomeres and aging. Physiol Rev 2008;88: 557–79.
34. Gomez-Millan J, Goldblatt EM, Gryaznov SM, Mendonca MS, Herbert BS. Specific telomere dysfunction induced by GRN163L increases radiation sensitivity in breast cancer cells. Int J Radiat Oncol Biol Phys 2007;67:897–905.
35. Kanzawa T, Germano IM, Komata T, Ito H, Kondo Y, Kondo S. Role of autophagy in temozolomide-induced cytotoxicity for malignant glioma cells. Cell Death Differ 2004;11:448–57.
36. Ulasov IV, Sonabend AM, Nandi S, Khramtsov A, Han Y, Lesniak MS. Combination of adenoviral virotherapy and temozolomide chemotherapy eradicates malignant glioma through autophagic and apoptotic cell death *in vivo*. Br J Cancer 2009;100:1154–64.
37. Fu J, Liu ZG, Liu XM, et al. Glioblastoma stem cells resistant to temozolomide-induced autophagy. Chin Med J (Engl) 2009;122:1255–9.
38. Shammas MA, Koley H, Bertheau RC, et al. Telomerase inhibitor GRN163L inhibits myeloma cell growth *in vitro* and *in vivo*. Leukemia 2008;22:1410–8.
39. Ito H, Aoki H, Kuhnel F, et al. Autophagic cell death of malignant glioma cells induced by a conditionally replicating adenovirus. J Natl Cancer Inst 2006;98:625–36.
40. Dikmen ZG, Gellert GC, Jackson S, et al. *In vivo* inhibition of lung cancer by GRN163L: a novel human telomerase inhibitor. Cancer Res 2005;65:7866–73.

Clinical Cancer Research

The Telomerase Antagonist, Imetelstat, Efficiently Targets Glioblastoma Tumor-Initiating Cells Leading to Decreased Proliferation and Tumor Growth

Calin O. Marian, Steve K. Cho, Brian M. Mcellin, et al.

Clin Cancer Res 2010;16:154-163.